



School of Computing Computational PDEs Unit

COMPUTATIONAL ENGINEERING CHALLENGES FOR ADAPTIVE
MESH REFINEMENT

Chris Goodyer, Roger Fairlie, Daniel Hart

Martin Berzins

Thanks to Laurence Scales of Shell Global Solutions and Chris Johnson at Utah

This work is funded by EPSRC and by Shell Global Solutions.

University of Utah CSAFE DoE Project– Yr 5 Demo

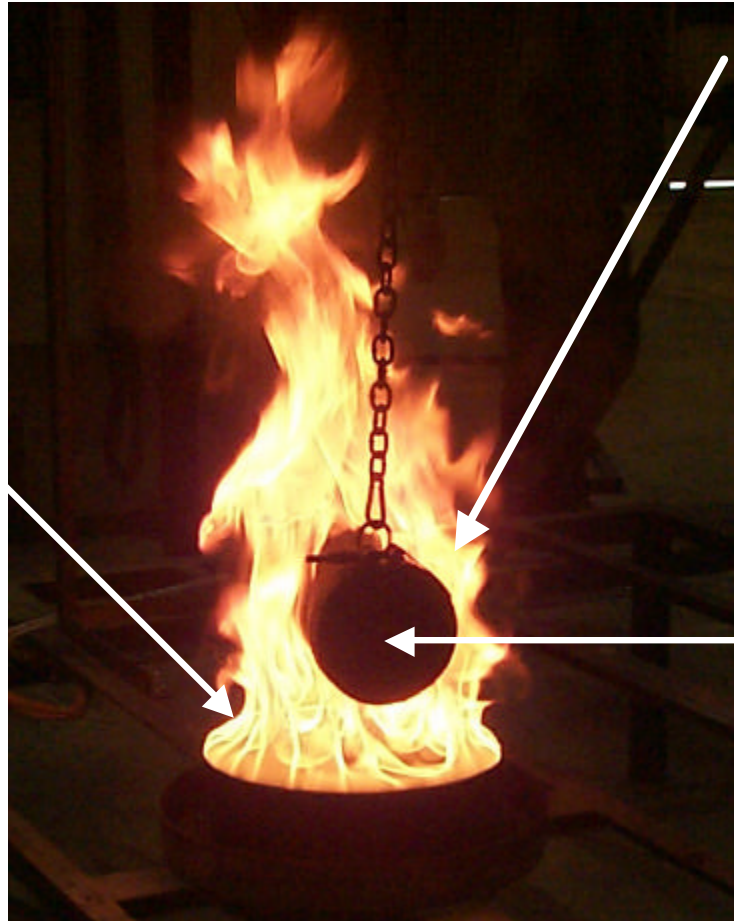
Pershing, Smith, McMurtry, Johnson, Parker et al.

When is the explosion?
How strong is it ?

Hydrocarbon Fire

- turbulent combustion
- complex kinetics
- soot formation
- wind allowed
- wide range of scales

ARCHES CODE



Metal Container

- heat transfer from fire
- fragmentation

MPM/ICE CODE

HE Material PBX

- surface burning
- microscopic crack formation

Mesh adaptation, large-scale parallelism, PSEs **Uintah**, viz, validation

MODELLING ELASTOHYDRODYNAMIC LUBRICATION (EHL)

Background 10 % GNP cost of friction/wear

- Valves/piston rings/gearboxes have pressures exceeding 1GPa!
- Viscosity of lubricant at 0.5GPa 10^6 times atmospheric value
- Lubricants become glass-like at 2-4 GPa - metal deforms
- Integro-differential model, Transient, non-Newtonian, thermal, with Cavitation at exit - free boundary
- Real surfaces are rough on very different scales
- Need to match computations to experiments as part of design studies
- Key quantities are friction and minimum film thickness

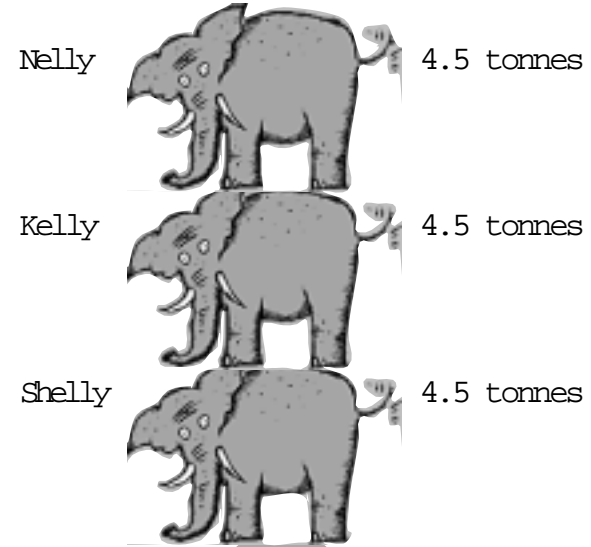
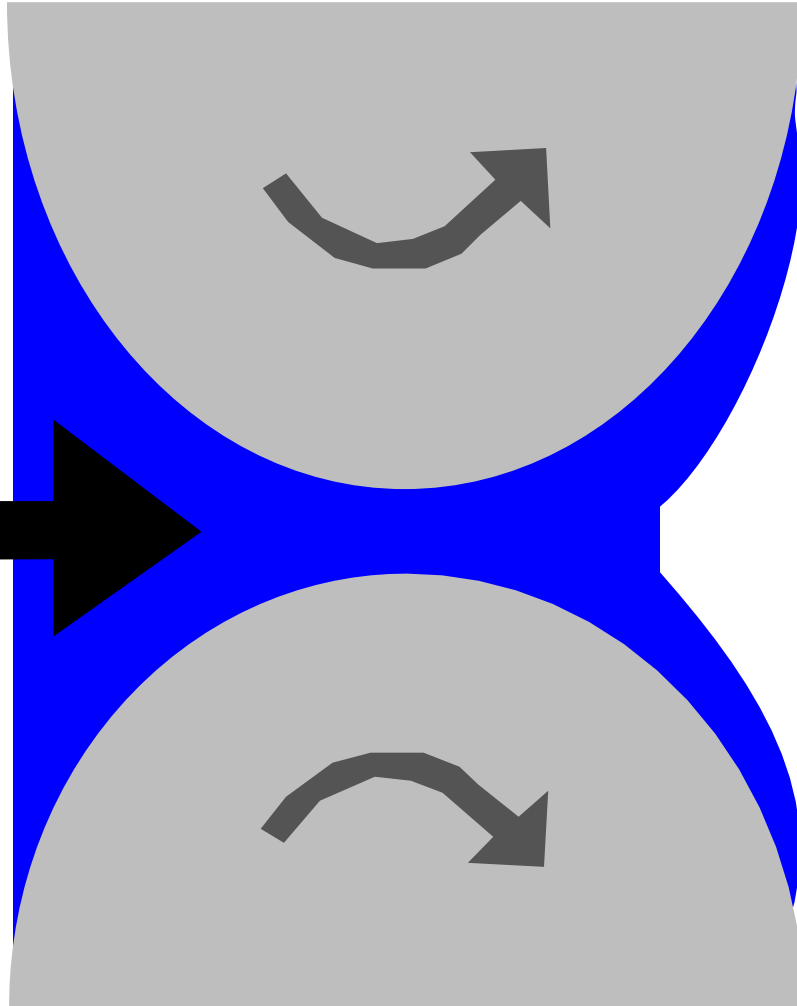
CSAFE and EHL Common Themes

- Complex and/or experimental mathematical models, beyond analysis?
- Inherently transient with multiple space and time scales
- Only tractable with use of multigrid type speedups and parallelism
- Accuracy requirements in terms of user quantities of interest
- Grid adaptation on cartesian meshes used to resolve scales
- Requirement for Problem Solving Environments
- Computing any reasonable solution is a challenge

Talk outline

- What is elastohydrodynamic lubrication?
- Governing equations and theory
- The 1D line contact problem
 - Discretisation and multilevel methods
 - Grid adaptation, errors, reference solutions
 - Example adaptive thermal roughness results
- The 2D circular contact problem
- Solving transient problems, reversal, roughness
- Future work

A hydrodynamic contact

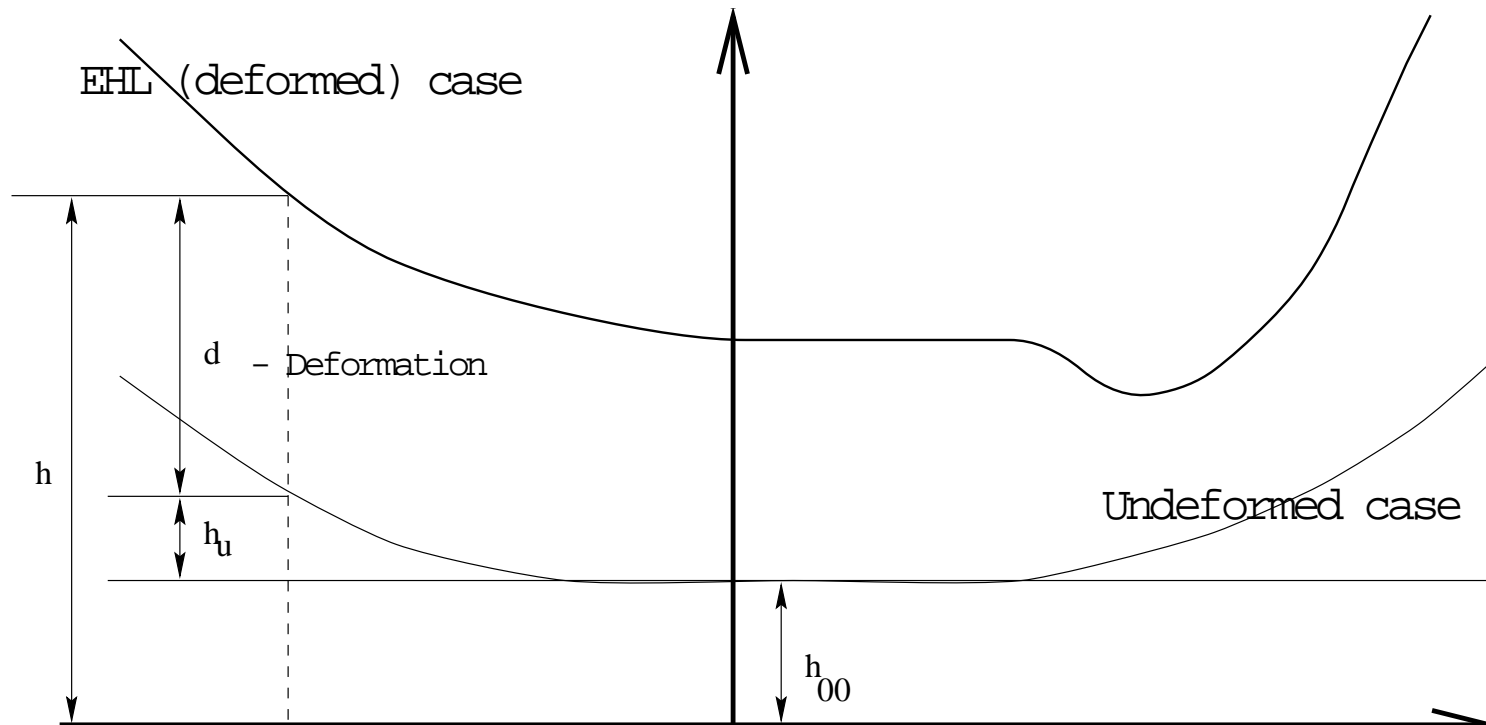


Contact Area 45 mm^2

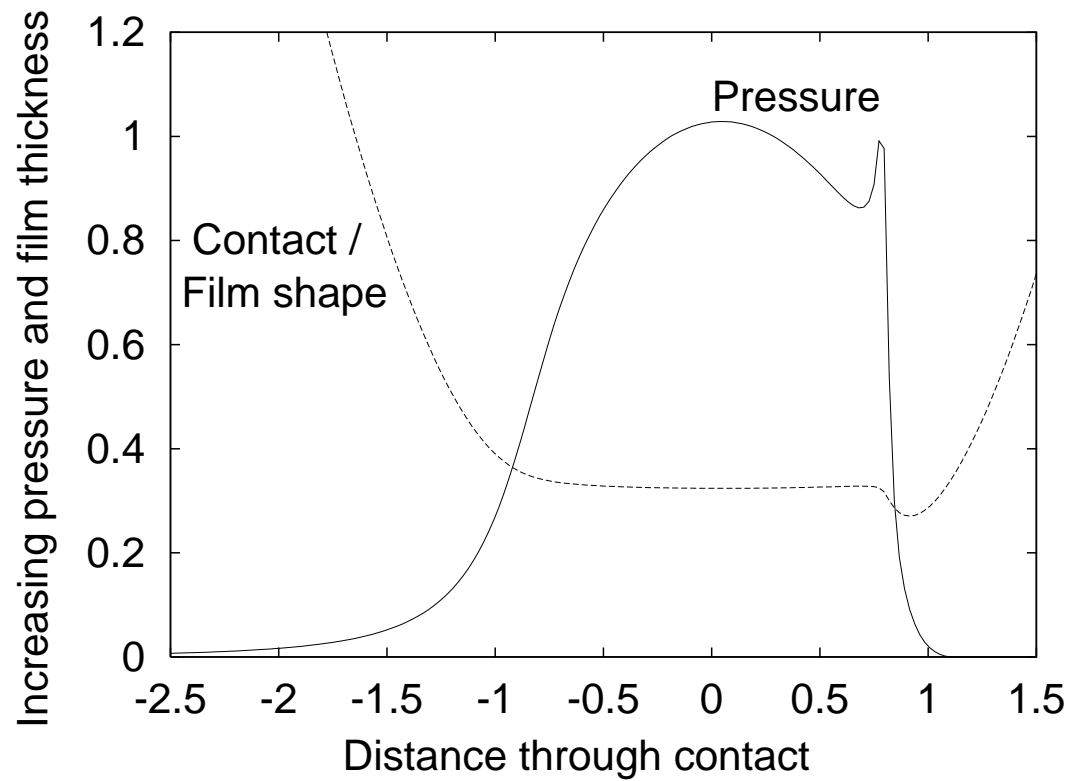
Applied load of
3 GPa

$$1 \text{ Gpa} = 100 \text{ Kg/mm}^2$$

(Elasto)hydrodynamic Lubrication Contacts



Geometry and Pressure plots across an EHL contact



Governing Equations I: The Reynolds Equation

$$\frac{\partial}{\partial x} \left(\frac{\rho h^3}{\eta} \frac{\partial p}{\partial x} \right) + \frac{\partial}{\partial y} \left(\frac{\rho h^3}{\eta} \frac{\partial p}{\partial y} \right) = 6 \left\{ u_s \frac{\partial (\rho h)}{\partial x} + v_s \frac{\partial (\rho h)}{\partial y} + \rho h \frac{\partial u_s}{\partial x} + \rho h \frac{\partial v_s}{\partial y} + 2 \frac{\partial (\rho h)}{\partial t} \right\}$$

where,

p is the pressure, h is the film thickness, η is the viscosity,

ρ is the density, t is the time, x, y Cartesian coordinates

and u_s, v_s are the surface velocities in the x and y directions respectively.

Equation changes type in contact region from parabolic to hyperbolic.

Governing Equations II: Film Thickness Equation

1D line contact:

$$h(x, y) = h_{00} + \frac{x^2}{2R_x} + \frac{4}{\pi E'} \int_{-\infty}^{\infty} \ln \left| \frac{x - x'}{x_0} \right| p(x') dx'$$

2D circular point contact:

$$h(x, y) = h_{00} + \frac{x^2}{2R_x} + \frac{y^2}{2R_y} + \frac{2}{\pi E'} \int_{-\infty}^{\infty} \int_{-\infty}^{\infty} \frac{p(x', y') dx' dy'}{\sqrt{(x - x')^2 + (y - y')^2}},$$

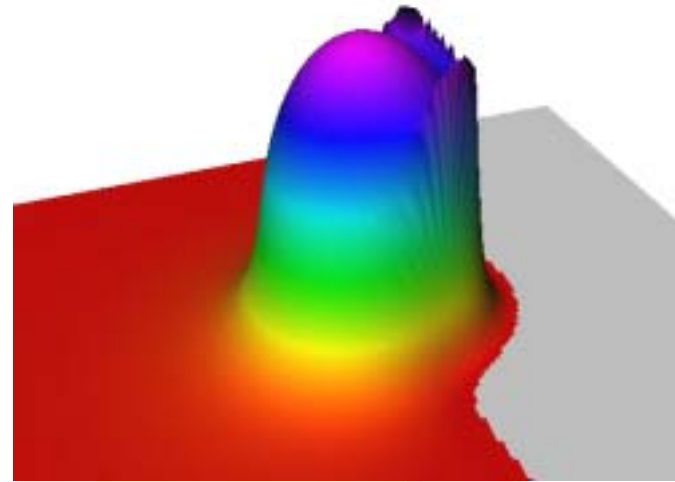
Film thickness, h , at a point depends upon all pressures! $O(N_x^2 N_y^2)$!

Conservation law - applied load carried entirely by lubricant film:

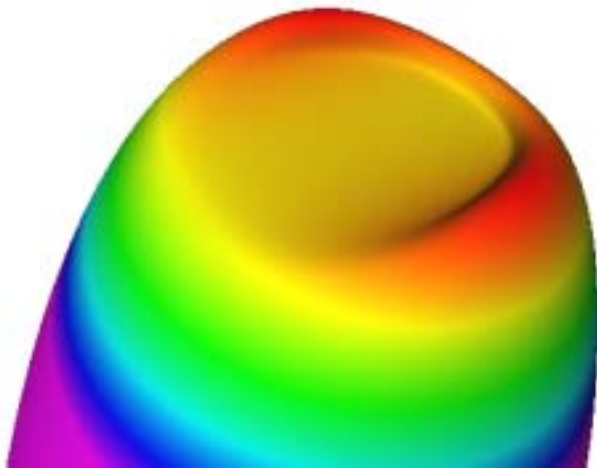
$$\int_{-\infty}^{\infty} \int_{-\infty}^{\infty} p(x, y) dx dy = F$$

Surface Roughness replace $\frac{x^2}{2R_x} + \frac{y^2}{2R_y}$ with real surface profile.

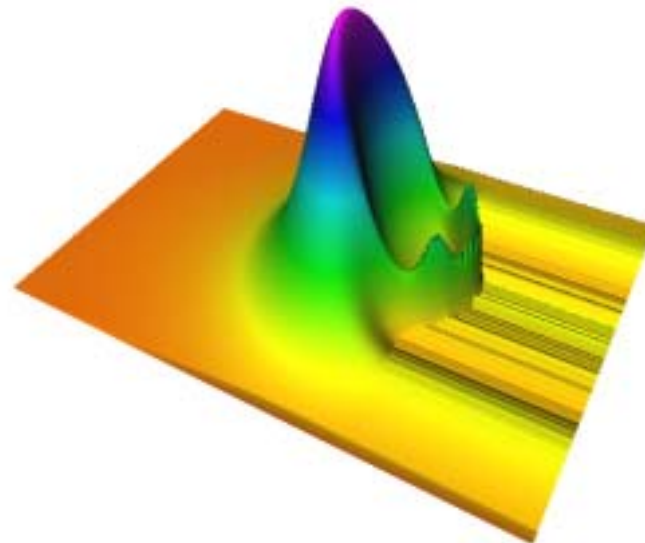
Typical solutions



Pressure



Film thickness



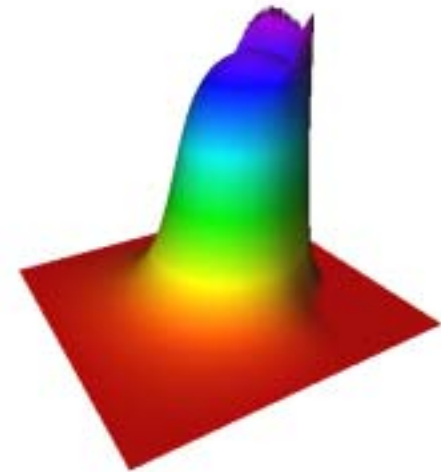
Temperature

Isothermal Model: Density and Viscosity Variation

Density model: (Dowson and Higginson)

$$\rho(p) = \rho_0 \left(1 + \frac{5.8 \times 10^{-10} p}{1 + 1.7 \times 10^{-9} p} \right)$$

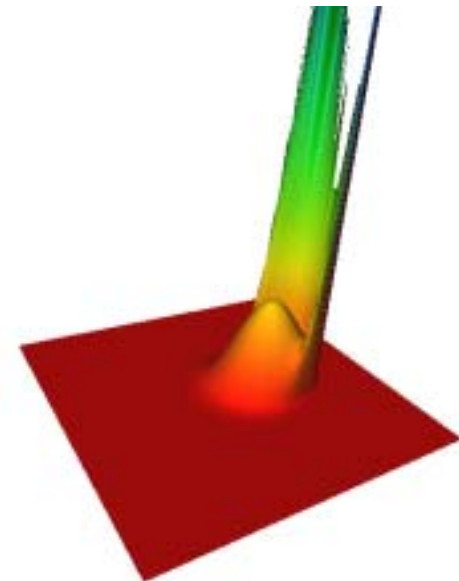
[Pictured non-dimensional range 1 → 1.16]



Viscosity Model: (from Roelands equation)

$$\eta(p) = \eta_0 \exp \left\{ \frac{\alpha p_0}{z} \left[-1 + \left(1 + \frac{p}{p_0} \right)^z \right] \right\}$$

[Pictured non-dimensional range 1 → 13300]



- More realistic rheological (non-Newtonian models) are now used instead

Governing Equations IV - The Energy Equation

For thermal cases the Energy Equation also applies:

$$\rho \left\{ \frac{1}{2} \frac{\partial \theta}{\partial T} + U_m \frac{\partial \theta}{\partial X} + V_m \frac{\partial \theta}{\partial Y} + \frac{\theta - \theta_b}{H} \left[(U_m - U_b) \frac{\partial H}{\partial X} + V_m \frac{\partial H}{\partial Y} \right] \right\} =$$

$$\frac{3k}{2B^2H^2} (\theta_a + \theta_b - 2\theta) + \beta_e \theta \left(\frac{1}{2} \frac{\partial P}{\partial T} + U_m \frac{\partial P}{\partial X} + V_m \frac{\partial P}{\partial Y} \right) -$$

$$2B\mu \left[\left(U_m - \frac{U_e}{2} \right) \frac{\partial P}{\partial X} - V_m \frac{\partial P}{\partial Y} \right] + \frac{B\mu\kappa}{3} \eta \Gamma_m^2$$

with the two surface temperatures given in the form

$$\theta_a(X) = 1 + 2\kappa\chi_a \int_{-\infty}^X \frac{(3\theta - 2\theta_a - \theta_b) d\zeta}{H(X) \sqrt{X - \zeta}}$$

Theoretical Results of Oden and Wu (1985) (1987)

Formulate simplified steady isothermal problem as variational inequality.

$$A : p \rightarrow -\nabla \cdot (h^3(p) e^{-\alpha p} \nabla p) + c \frac{\partial u h}{\partial x}$$

Treat cavitation by including penalty term (comp. equiv to setting p zero)

$$\Phi(p) = (p - |p|)/(2\varepsilon), \quad \varepsilon > 0$$

Cast FE method as

$$\langle A(p_\varepsilon), q \rangle + \langle \Phi(p_\varepsilon), q \rangle = 0, \quad \forall q \in H_0^1(\Omega)$$

Oden and Wu prove there is a unique solution p_ε and that FEM solution p_ε^n converges to true solution.

$$\|p_\varepsilon - p_\varepsilon^n\|_{H^1} \leq C \Delta x |p_\varepsilon|_{H^2}$$

Error $O(\Delta x^2)$ for p_ε, h in L_2 norm. **LIGHTLY LOADED** cases only

Line Contact - Discretisation

The Reynolds Equation:

$$\frac{1}{\Delta T} (\bar{\rho}_i H_i - \bar{\rho}_i^{t-1} H_i^{t-1}) = \frac{1}{\Delta X^2} \left(\varepsilon_{i+\frac{1}{2}} (P_{i+1} - P_i) - \varepsilon_{i-\frac{1}{2}} (P_i - P_{i-1}) \right)$$

$$- \frac{1}{\Delta X} (\bar{\rho}_i H_i - \bar{\rho}_{i-1} H_{i-1}) \quad \text{where} \quad \varepsilon_i = \frac{\bar{\rho}_i H_i^3}{\bar{\eta}_i \bar{\lambda}}$$

The Film Thickness Equation:

$$H_i = H_{00} + X_i^2 - \frac{1}{\pi} \sum_{j=1}^n K_{ij} P_j \quad \text{where}$$

$$K_{ij} = (i - j + \frac{1}{2}) \Delta X (\ln(|i - j + \frac{1}{2}| \Delta X) - 1) - (i - j - \frac{1}{2}) \Delta X (\ln(|i - j - \frac{1}{2}| \Delta X) - 1)$$

The Force Balance Equation:

$$\Delta X \sum_{i=1}^n P_i = \frac{\pi}{2}$$

Second order upwind $\partial h / \partial x$ doesn't produce expected improvement

Line Contact - Thermal Density and Viscosity

The Density Equation:

$$\rho_i = \rho_0 \left(1 + \frac{\mu p_i}{1 + \nu p_i} \right) \{ 1 - \beta_e(p_i)(\theta_i - \theta_0) \}$$

where $\beta_e(p_i) = \beta_{e,0} \exp(-\kappa_e p_i)$

The Viscosity Equation:

$$\eta = \eta_0 \exp \left(\frac{\alpha_0 p_0}{z_0} \left\{ \left(1 + \frac{p_i}{p_0} \right)^{z(\theta)} \left(\frac{\theta_i - \theta_r}{\theta_0 - \theta_r} \right)^{-s} - 1 \right\} \right)$$

where $z(\theta) = z_0 - z_1 \ln \left(\frac{\theta_i - \theta_r}{\theta_0 - \theta_r} \right)$

and $s = \frac{\beta_0 z_0}{\alpha_0 p_0} (\theta_0 - \theta_r)$

Line Contact Discretisation - Energy Equation

$$\bar{\rho}_i \left\{ \frac{(\theta_i^{t_n} - \theta_i^{t_{n-1}})}{2\Delta T} + U_m \frac{(\theta_i - \theta_{i-1})}{\Delta X} + \frac{(\theta_i - \theta_b)}{H} \left((U_m - U_b) \frac{H_i - H_{i-1}}{\Delta X} \right) \right\} =$$

$$\frac{3k}{2B^2 H_i^2} (\theta_a + \theta_b - 2\theta_i) + \beta_e \theta_i \left(\frac{(P_i^{t_n} - P_{i-1}^{t_{n-1}})}{2\Delta T} + U_m \frac{(P_i - P_{i-1})}{\Delta X} \right) -$$

$$2B\mu \left(U_m - \frac{U_e}{2} \right) \frac{(P_i - P_{i-1})}{\Delta X} + \frac{B\mu\kappa}{3} \eta_i \Gamma_m^2$$

where

$$U_m = -\frac{H_i^2}{2\kappa\eta_i} \frac{(P_i - P_{i-1})}{\Delta X} + \frac{U_e}{2}.$$

The Surface Temperature Equation:

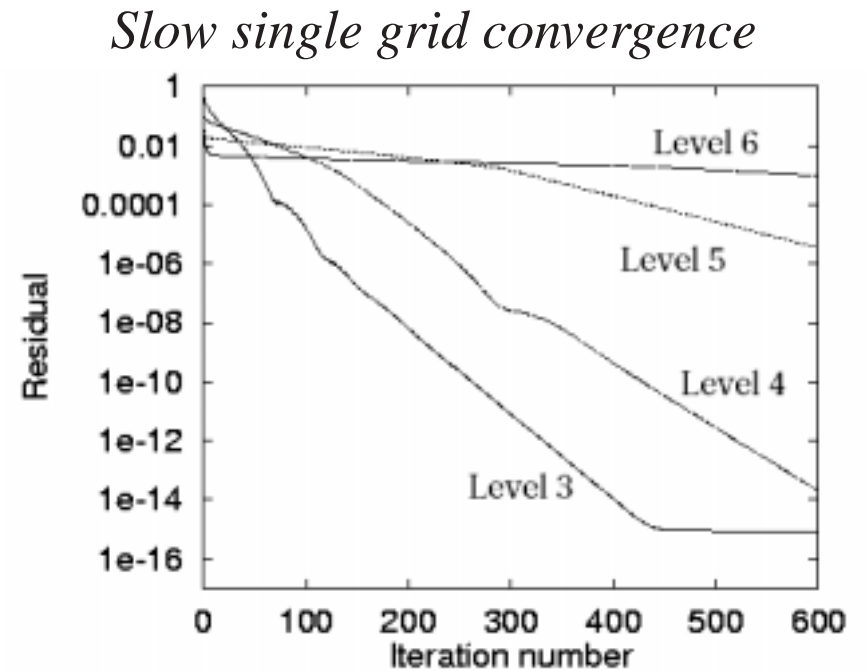
$$\theta_{a;i} = 1 + 4\kappa\chi_a \sum_{j=1}^i \left[\frac{\theta_{A;j-1} + \theta_{A;j}}{H_{j-1} + H_j} \left(\sqrt{X_j - X_{j-1}} - \sqrt{X_i - X_j} \right) \right]$$

Line Contact - Solution Methods

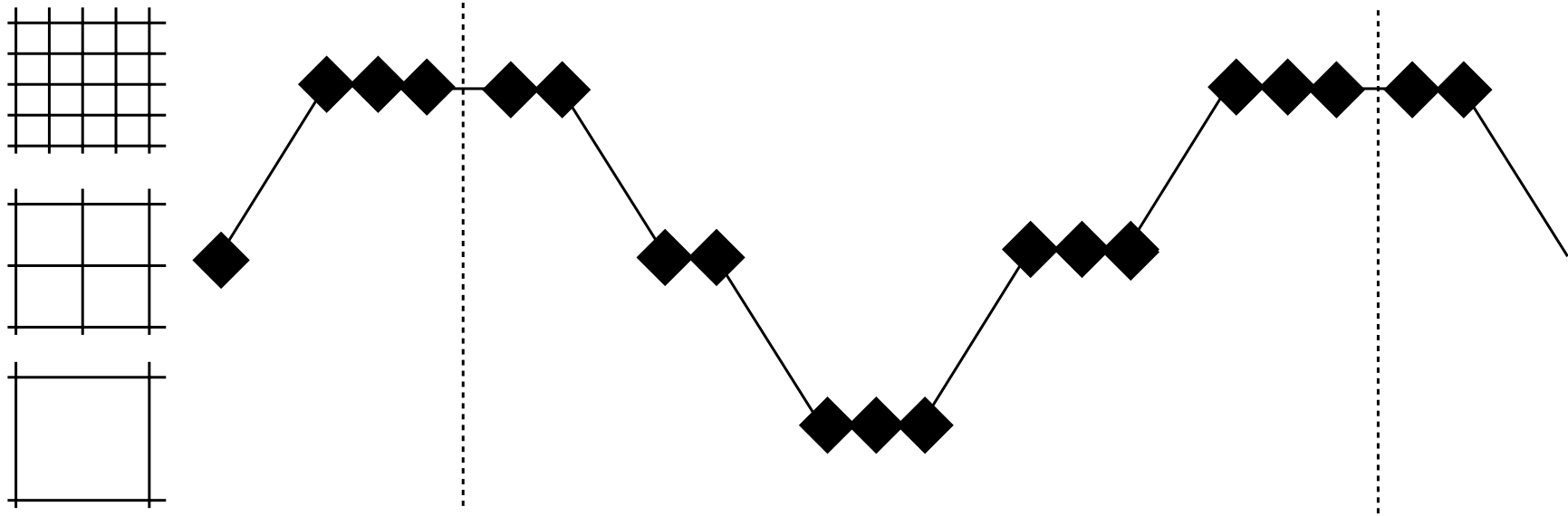
- Solve (non-linear) Reynolds equation for new Pressure
 - Use finite differences
 - Gauss-Seidel updates for whole line
 - Cavitation Region - Reynolds Equation not valid
- Update H using new P
 - Computationally expensive but Multi-level Multi-integration substantially reduces work
- Update Density and Viscosity
- Pointwise Jacobi scheme used to solve Energy Equation

Line Contact - Multigrid [Lubrecht and Venner]

- Standard iterative methods good at removing high frequency errors relative to grid
- Bad at removing low frequency errors relative to grid
- Use of multiple levels of grid refinement accelerate convergence on fine grids
- On fine meshes more of the errors are low frequency relative to grid



Multigrid Cycles

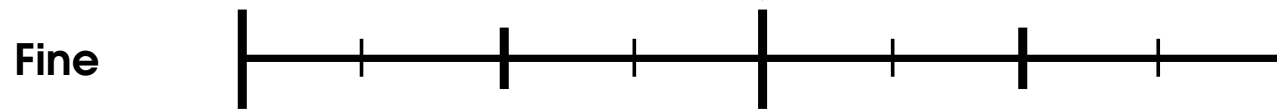


Adaptive multigrid is used in practice.

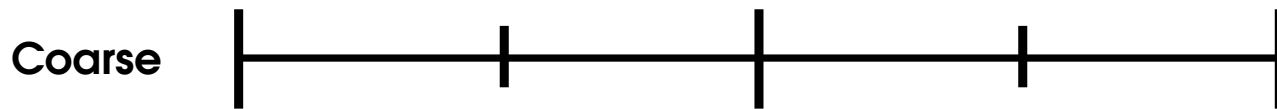
Multi-Level Multi-Integration

$$h_i = \sum k_{|i-j|} P_j$$

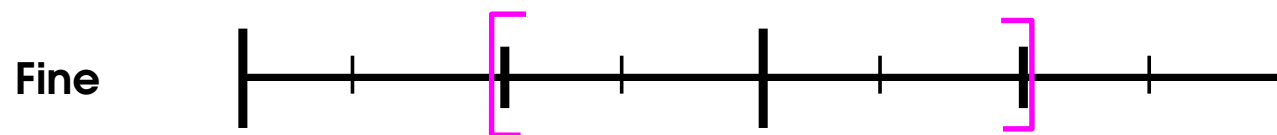
1. Given P_i and k_i



2. 6th order restriction of P and k and then sum on coarsest grid



3. 6th order prolongation of coarse grid integrals to fine grid

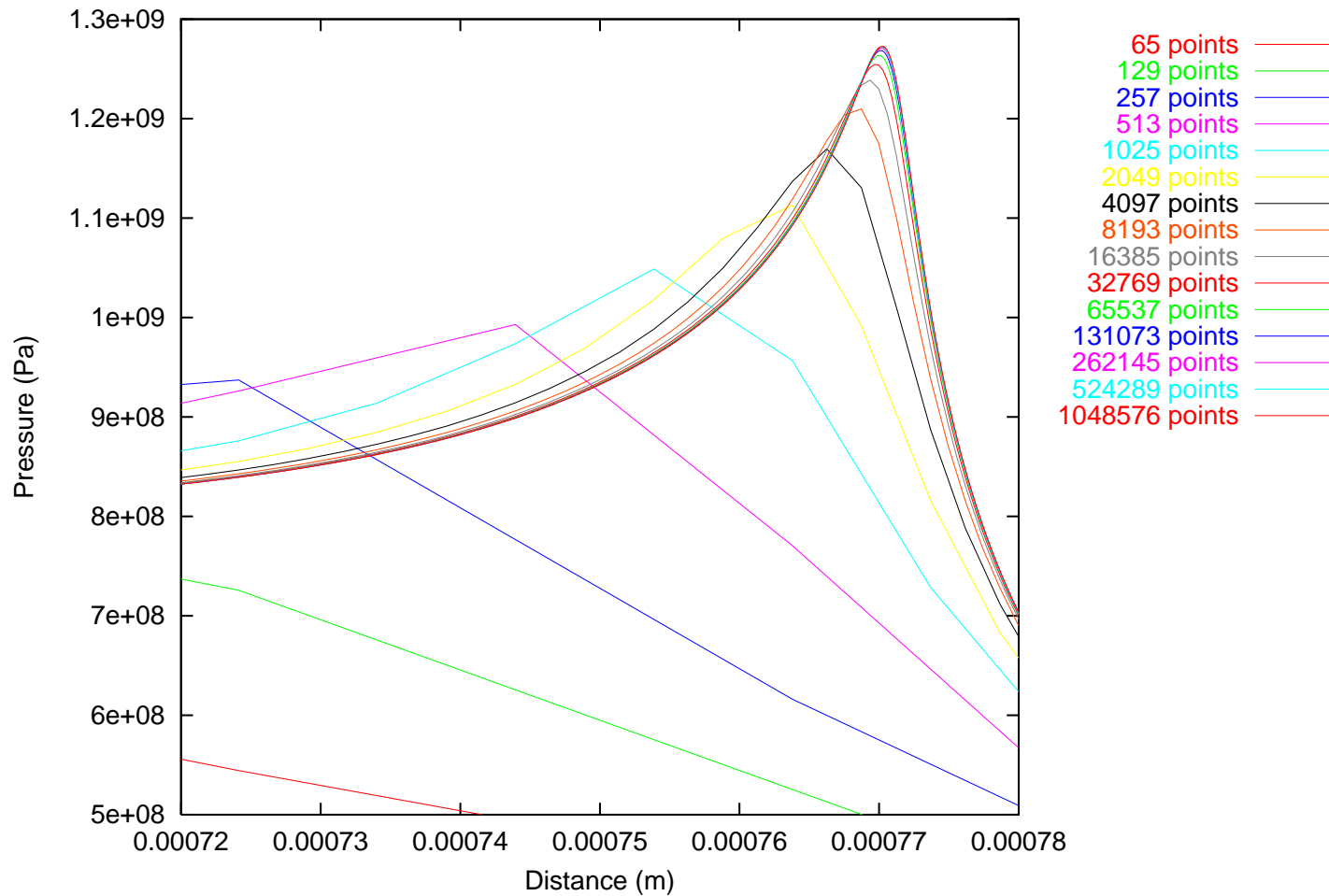


4. Correct solution in zone around singularity at x_i

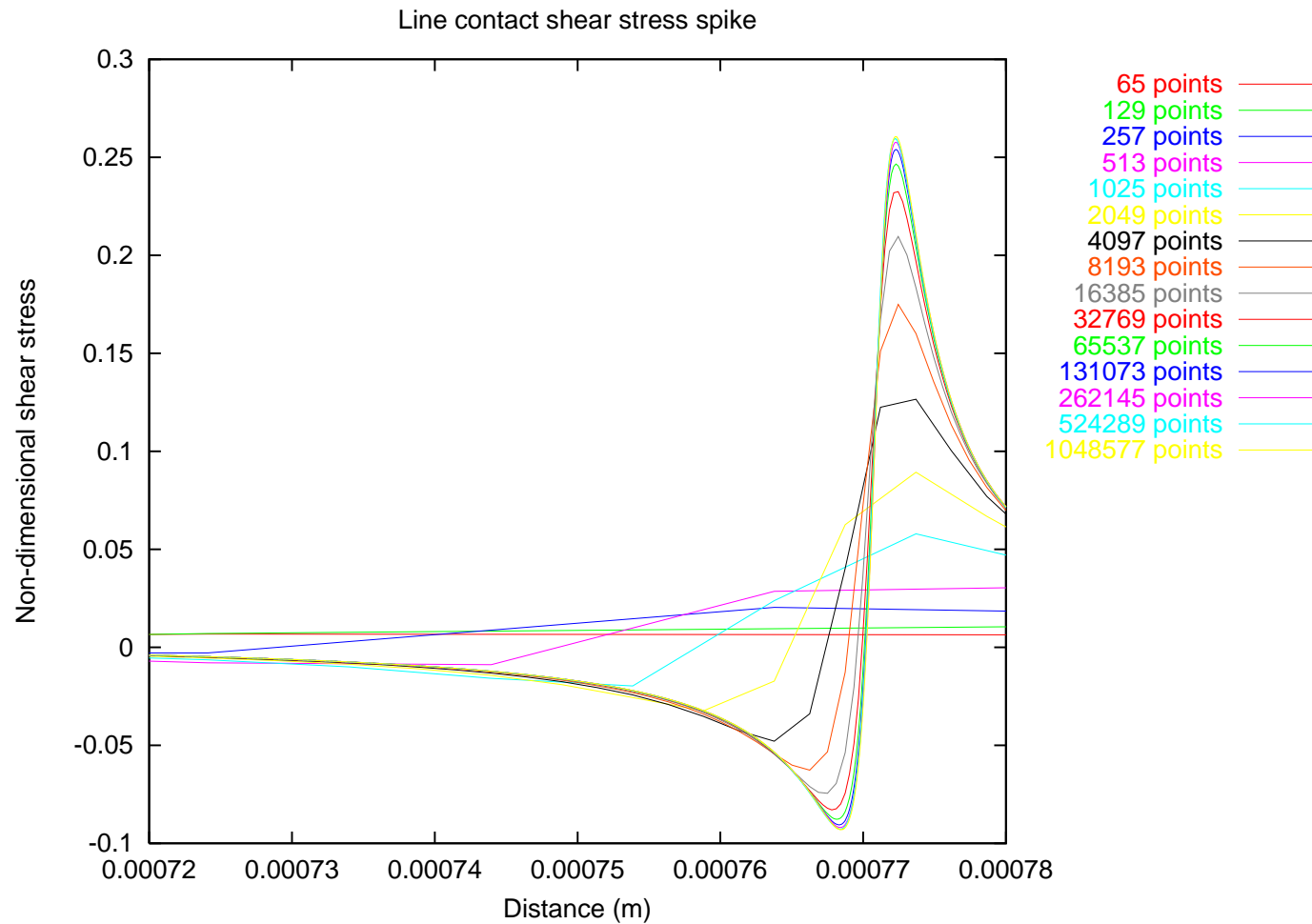
For N_x h_i fine grid points the calculation is $O(N_x \log N_x)$ not $O(N_x^2)$

Computational Reference Solutions: Pressure

calculated on grid 19 mesh 10^6 grid points. Pressure spike is smooth.



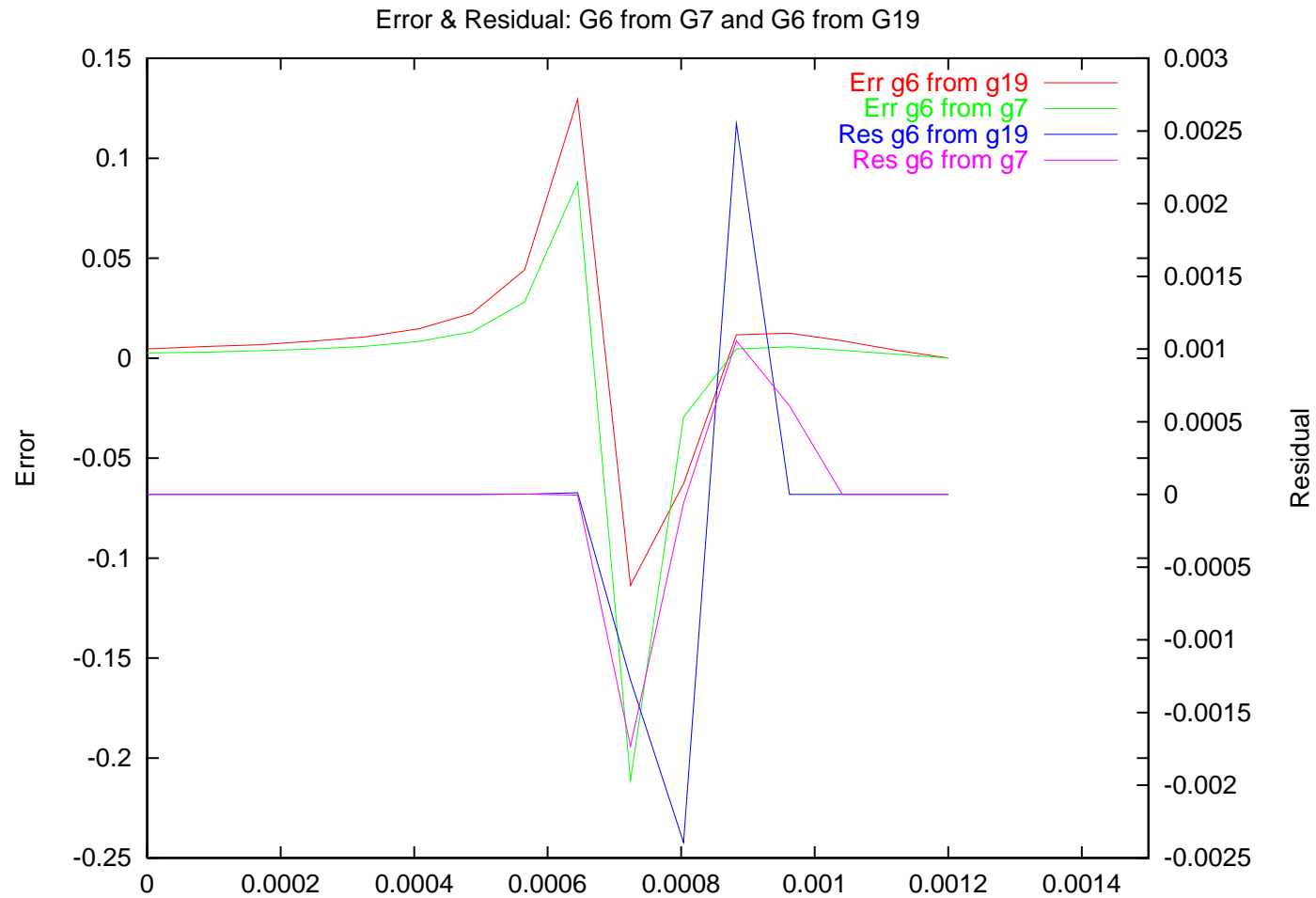
Computational Reference Solutions: Shear Stress



Stress - $\partial p / \partial x$ - harder to resolve than p .

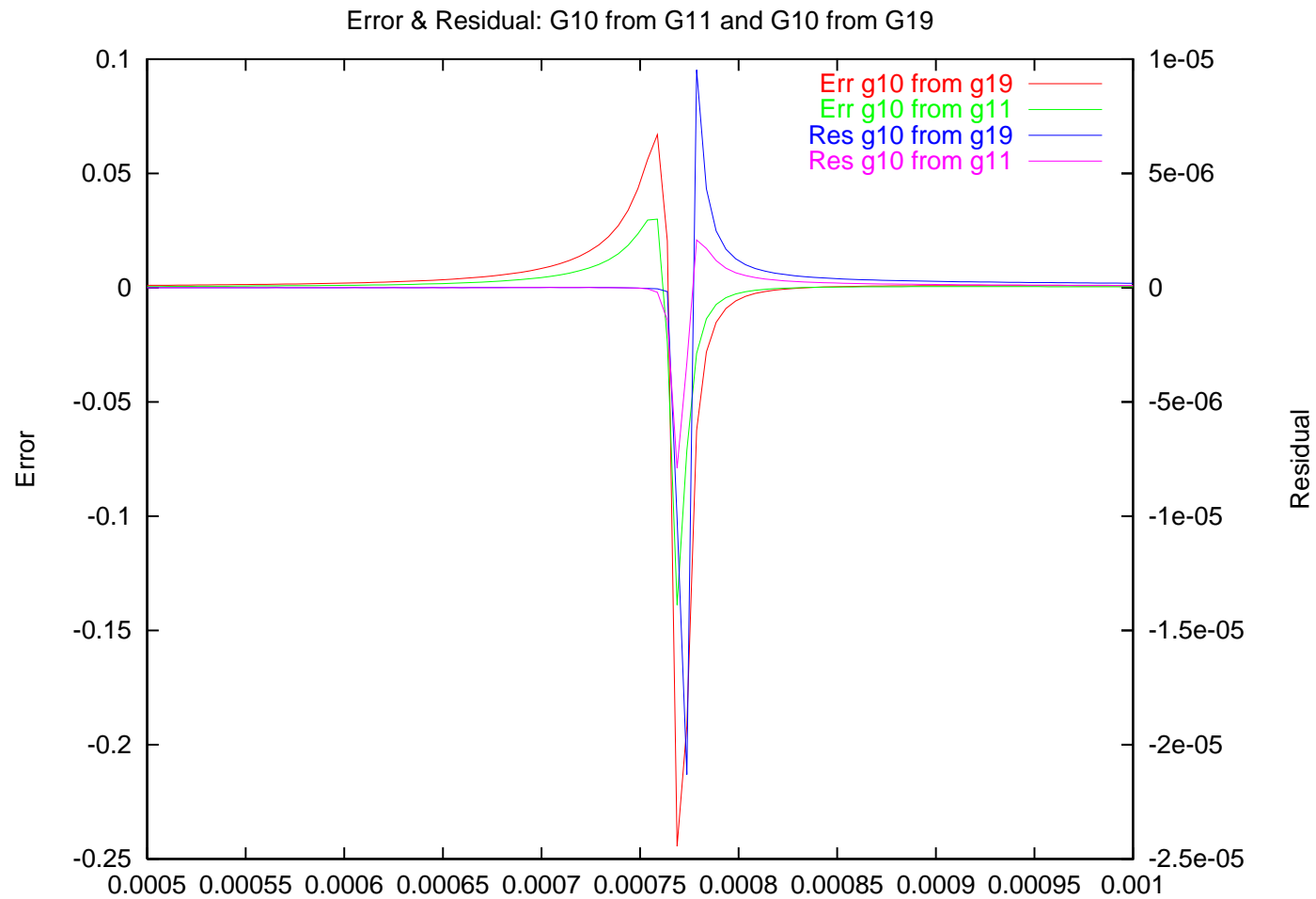
Error Indicators: Coarse Mesh 257 pts

Two possible approaches residual-based and extrapolation-based



Error Indicators: Medium Mesh 2045 pts

Two possible approaches residual-based and extrapolation-based

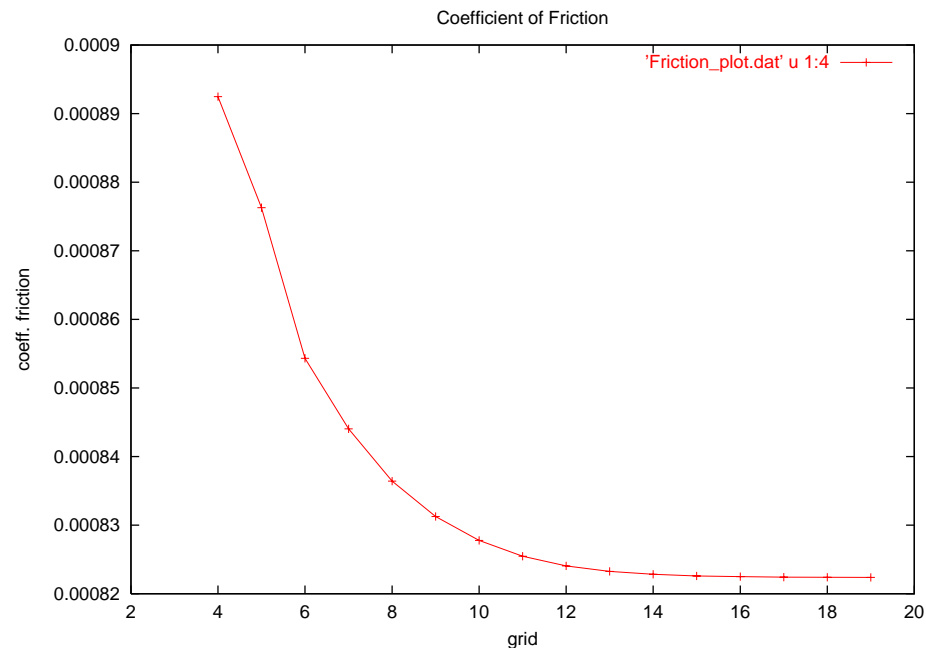


Quantities of Interest

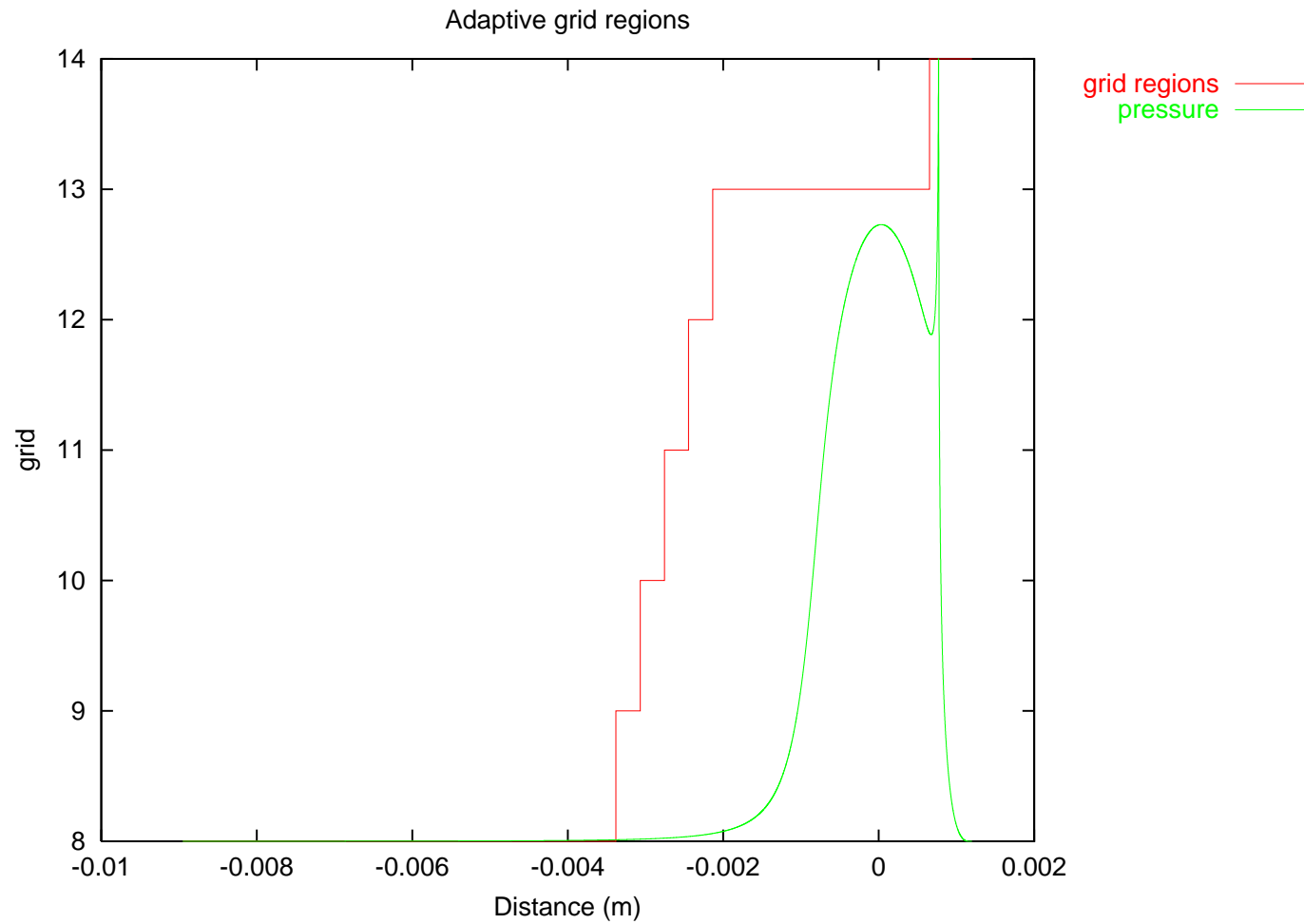
Minimum film thickness - how much of a gap is there?

Coefficient of friction - integral of shear stress F_b or F_a where e.g.

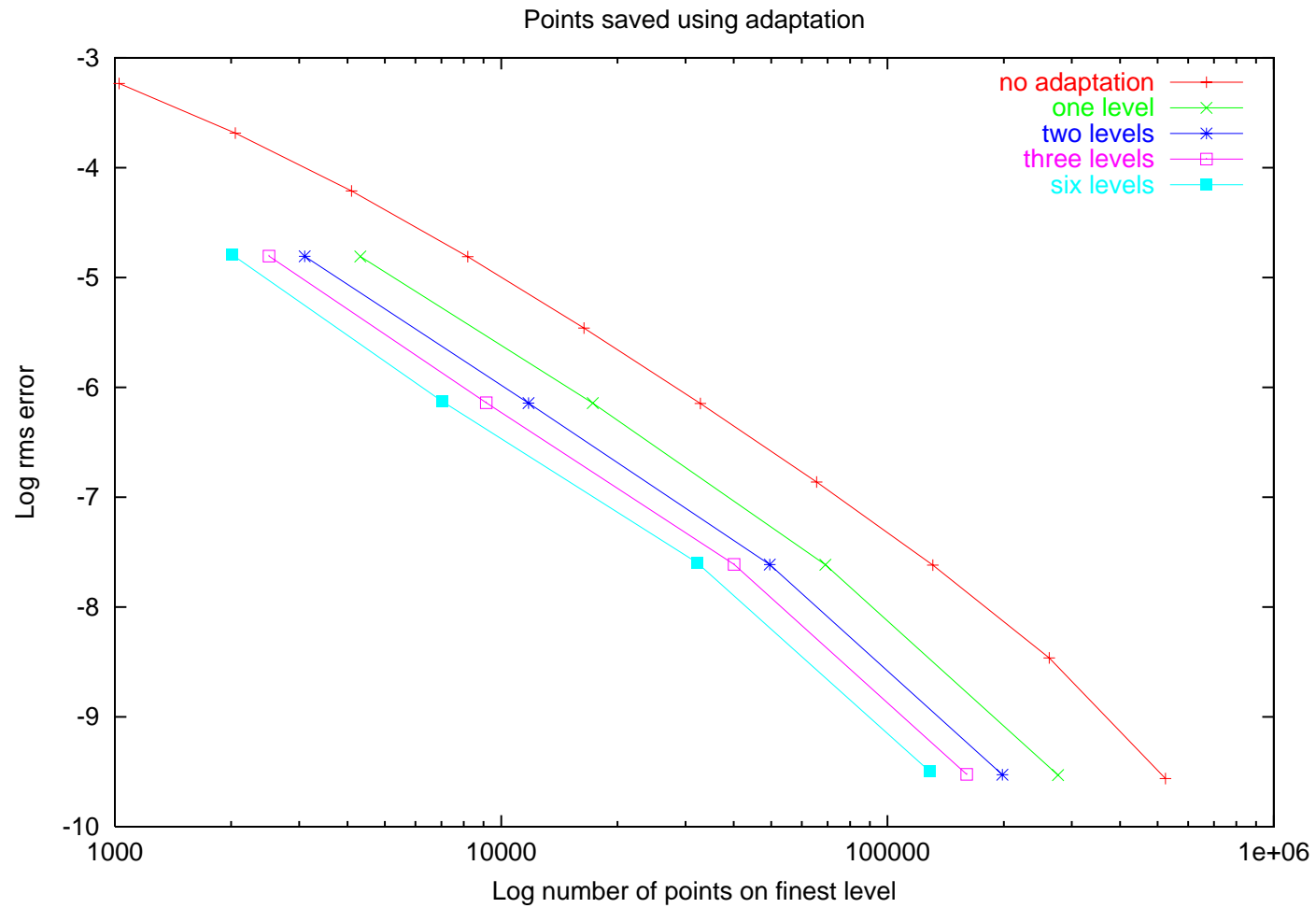
$$F_b = \int_{xmin}^{xmax} \frac{h(x)}{2} \frac{\partial p}{\partial x} + \frac{\eta(x)}{h(x)} (U_b - U_a) dx$$



Line Contact - Adaptive Mesh Solutions.



Line Contact - Adaptive Mesh vs Fixed Mesh.

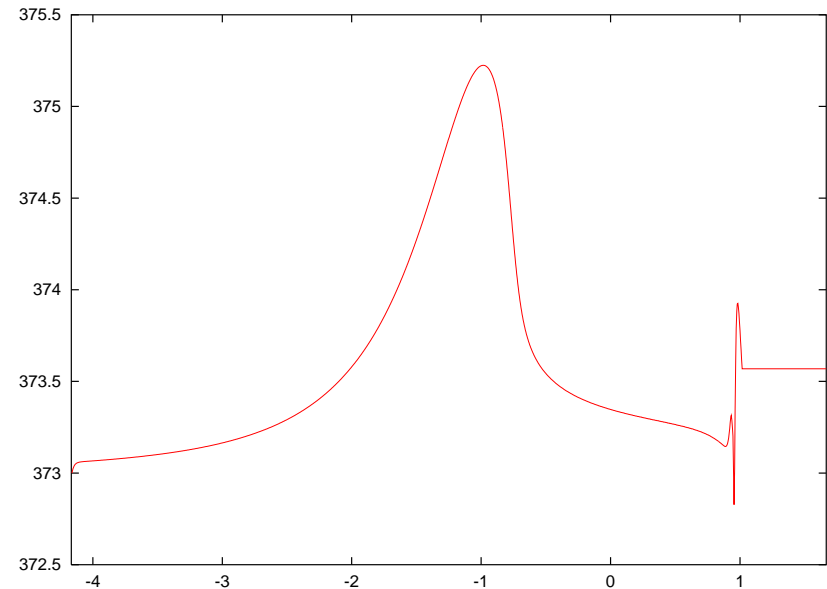


Line Contact - Thermal Effects

Thermal cases are important because there can be a significant temperature increase - up to 100° across the contact. This affects the friction in the contact.

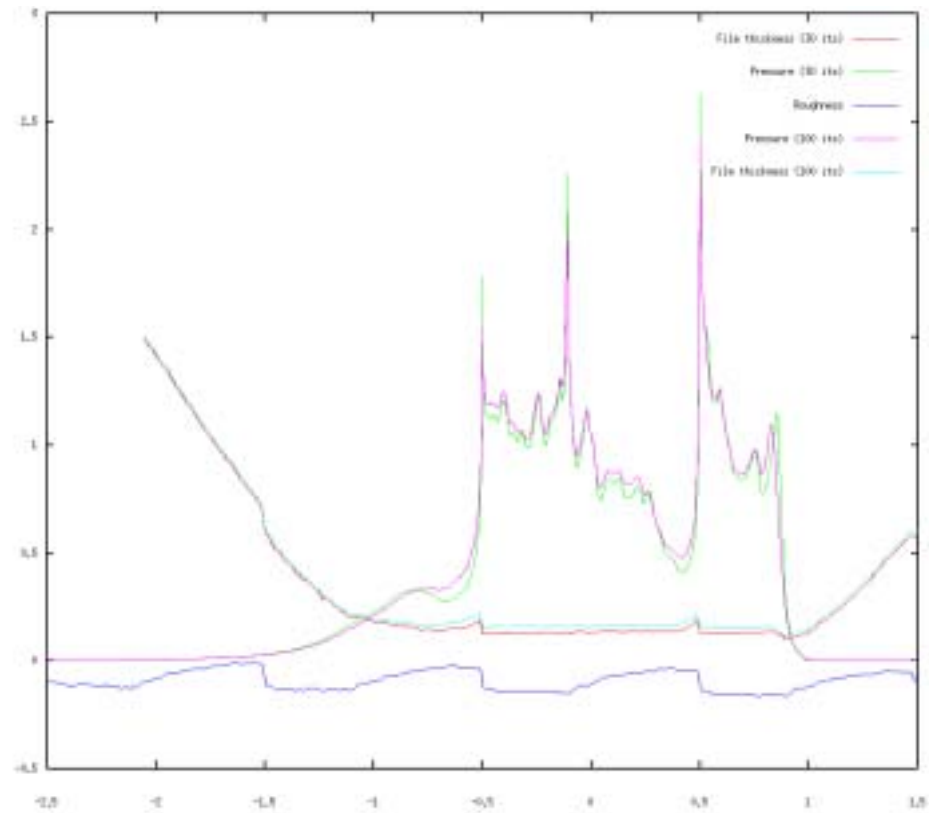
The extent of these changes is governed by the type of lubricant being used, the fluid velocity etc

Temperature across domain



Surface Roughness Effects

Real surfaces are not smooth. Surface geometry can now be measured.



Point Contact - 2D Discretisation

Reynolds and energy equations discretised using central/upwind f.d.
(May also be viewed as bilinear finite element method)

$$\text{Film Thickness : } H_{i,j} = H_{00} + \frac{X_i^2}{2} + \frac{Y_j^2}{2} - \frac{2}{\pi^2} \sum_{k=1}^{N_X} \sum_{l=1}^{N_Y} K_{i,j,k,l} P_{k,l}$$

$$\text{where } K_{i,j,k,l} = \frac{2}{\pi^2} \left\{ \begin{aligned} &|X_p| \sinh^{-1} \left(\frac{Y_p}{X_p} \right) + |Y_p| \sinh^{-1} \left(\frac{X_p}{Y_p} \right) \\ &- |X_m| \sinh^{-1} \left(\frac{Y_p}{X_m} \right) - |Y_p| \sinh^{-1} \left(\frac{X_m}{Y_p} \right) \\ &- |X_p| \sinh^{-1} \left(\frac{Y_m}{X_p} \right) - |Y_m| \sinh^{-1} \left(\frac{X_p}{Y_m} \right) \\ &+ |X_m| \sinh^{-1} \left(\frac{Y_m}{X_m} \right) + |Y_m| \sinh^{-1} \left(\frac{X_m}{Y_m} \right) \end{aligned} \right\}$$

Point Contact - Energy Eqn Discretisation

$$\begin{aligned}
 \bar{\rho}_i & \left\{ \frac{\theta_{i,j} - \theta_{i,j}^{t_{n-1}}}{2\Delta T} + U_m \frac{\theta_{i,j} - \theta_{i-1,j}}{\Delta X} + \frac{\theta_{i,j} - \theta_b}{H_{i,j}} \left[(U_m - U_b) \frac{H_{i,j} - H_{i-1,j}}{\Delta X} + V_m \frac{H_{i,j} - H_{i,j-1}}{\Delta Y} \right] \right\} \\
 & = \frac{3k}{2B^2 H_{i,j}^2} (\theta_a + \theta_b - 2\theta_{i,j}) + \beta_e \theta_{i,j} \left[\frac{P_{i,j} - P_{i-1,j}^{t_{n-1}}}{2\Delta T} + U_m \frac{P_{i,j} - P_{i-1,j}}{\Delta X} + V_m \frac{P_{i,j} - P_{i,j-1}}{\Delta Y} \right] - \\
 & \quad 2B\mu \left[\left(U_m - \frac{U_e}{2} \right) \frac{P_{i,j} - P_{i-1,j}}{\Delta X} - V_m \frac{P_{i,j} - P_{i,j-1}}{\Delta Y} \right] + \frac{B\mu\kappa}{3} \eta_{i,j} \Gamma_m^2 \\
 \text{where } U_m & = -\frac{H_{i,j}^2}{2\kappa\eta_{i,j}} \frac{P_{i,j} - P_{i,j-1}}{\Delta X} + \frac{U_e}{2} \quad \text{and} \quad V_m = \frac{H_{i,j}^2}{2\kappa\eta_{i,j}} \frac{P_{i,j} - P_{i,j-1}}{\Delta Y}
 \end{aligned}$$

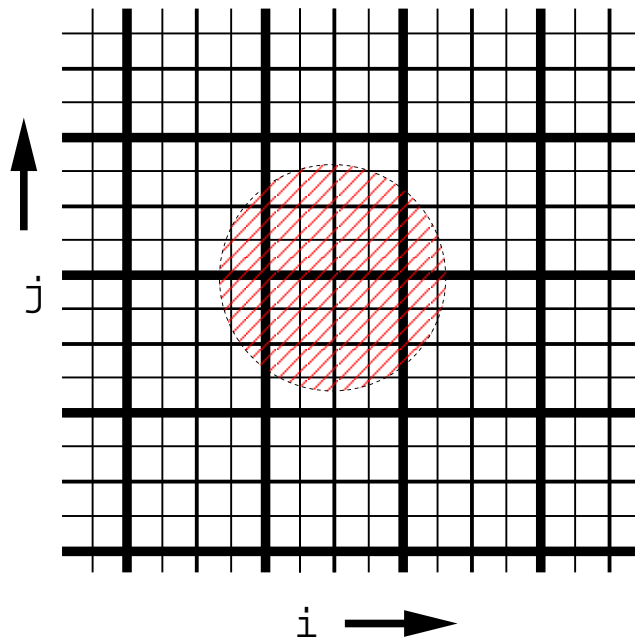
The Surface Temperature Equation:

$$\theta_{a;i,j} = 1 + 4\kappa\chi_a \sum_{k=1}^i \left[\frac{\theta_{A;k-1,j} + \theta_{A;k,j}}{H_{k-1,j} + H_{k,j}} \left(\sqrt{X_k - X_{k-1}} - \sqrt{X_i - X_k} \right) \right]$$

Point Contact - Solution methods

- Solve (non-linear) Reynolds equation for new Pressure
 - Contact Region solution schemes include:
 - * Distributive scheme [Lubrecht & Venner]
 - * Jacobi Line [Nurgat & Berzins]
 - Non-contact region - G-S Line scheme
 - Cavitation Region - Reynolds Equation not valid
- Update H using new P
 - Computationally expensive but Multilevel Multi-integration substantially reduces work
- Update Density and Viscosity
- Evaluate Energy Equation by pointwise Jacobi along each line

Point Contact - Multilevel Multi-Integration



- Aim is to reduce work by summing over as few elements as possible
- Sum over fine grid points near singularity
- Add sum from all coarse grid points
- Correct in region of influence

$$H_{i,j} = H_{00} + \frac{X_i^2}{2} + \frac{Y_j^2}{2} - \frac{2}{\pi^2} \sum_{k=1}^{N_x} \sum_{l=1}^{N_y} K_{i,j,k,l} P_{k,l}$$

This is similar to the fast multipole method $O(N_x \log(N_x) N_y \log(N_y))$

Point Contact - MLMI Speed-ups

MLMI computational times (s) for a single film thickness calculation

		Coarsest grid used in multi-integration				
		Level 3	Level 4	Level 5	Level 6	Level 7
Level	5	0.14	0.22	2.29	-	-
of	6	0.35	0.50	2.30	28.5	-
solution	7	1.14	1.26	3.21	28.2	397

Root mean square error of a typical calculation

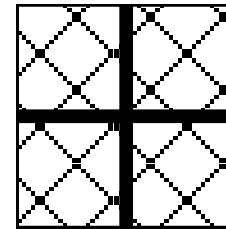
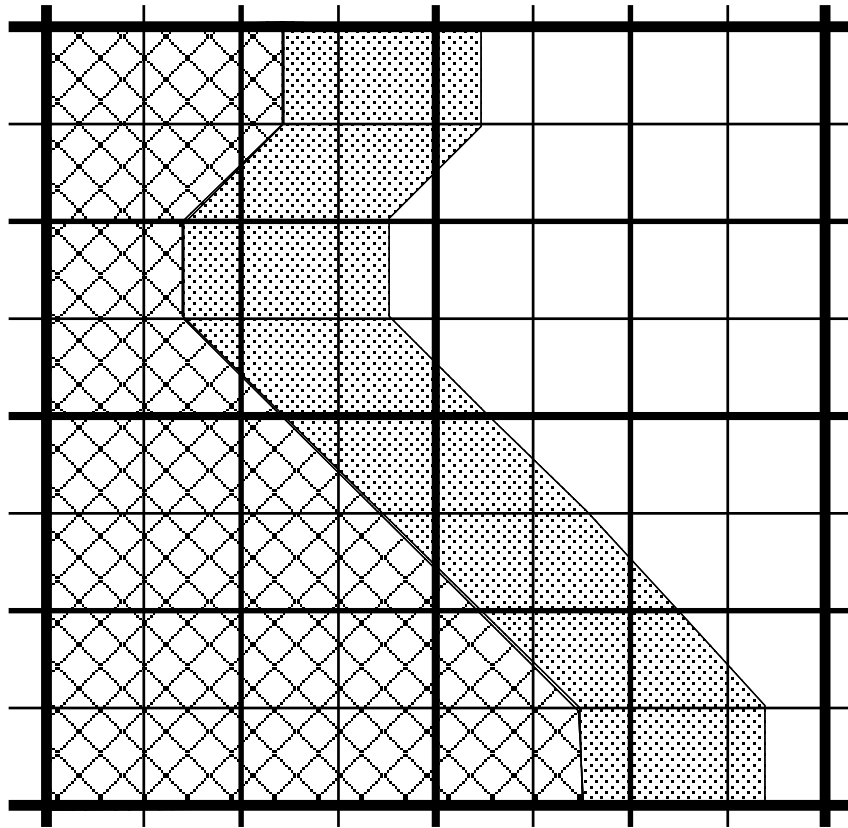
		Level 3	Level 4	Level 5	Level 6
Level	5	3.2×10^{-5}	1.2×10^{-5}	-	-
of	6	3.5×10^{-5}	1.8×10^{-5}	7.2×10^{-6}	-
solution	7	3.7×10^{-5}	2.1×10^{-5}	1.0×10^{-5}	3.8×10^{-6}

Point Contact Grid Adaptation

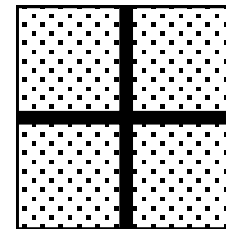
- EHL calculations are very expensive on fine meshes
- Interesting behaviour restricted to the contact area
- Inlet region very important for good solutions
- Adaptive meshing allows solutions of similar accuracy, but cheaper
- Given 1D results refine based on either:
 - pre-defined geometry
 - monitor function, e.g. residual or pressure
 - multilevel extrapolation error
- Work concentrated where needed

Deformation calculation not yet done on an adapted mesh

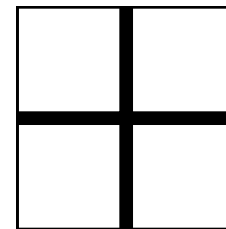
Grid Adaptation - Free boundary treatment



Pressure positive
point



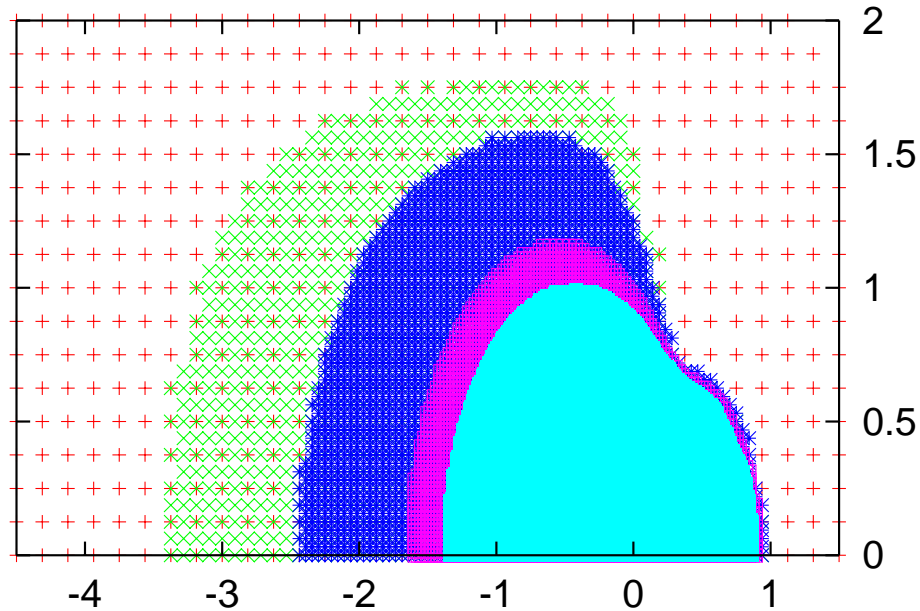
Cavitation point
included in
adaptive solve



Cavitation point
excluded from
adaptive solve

At least one point inside the cavitation region (zero pressure) included in each pressure solve

Grid Adaptation - Results



Grid dimension	Adaptation style	Speed up
129×129	Geometry	37.7%
257×257	Monitor function	49.9%
513×513	Error test	48.8%

Differential Algebraic Formulation of EHL

In discretised form, for solution vectors \underline{P} , \underline{H} and $\underline{\rho}$, the system can be written:

$$\text{Reynolds Equation: } \underline{F}(\underline{P}, \underline{\rho H}, [\underline{\rho \dot{H}}]) = 0$$

$$\text{Film thickness: } \underline{H} = \underline{h}_0 + K\underline{P}$$

K is a large dense block Toeplitz (non-singular?) matrix

There is no explicit transient derivative of pressure, hence this is not an ODE but a DAE system

Assuming non-singularity - this has DAE index 1

Transient EHL Problems

- EHL is an inherently transient field
- Novel use of a standard ODE solver coupled with standard convergence test linked to MG solver
- Continue iterations to reduce errors using Shampine convergence test:

$$\frac{\sigma}{1 - \sigma} \left\| \underline{H}^{(m+1)}(t_n) - \underline{H}^{(m)}(t_n) \right\| < 0.33tol$$

where tol is an error tolerance for the iteration, $\| \cdot \|$ a suitable norm, m the multigrid iteration number, and σ is an estimate of the rate of convergence

- Use of standard ODE techniques to predict next timestep solutions

Variable Time Stepping using Local Space/Time Error Control

Standard EHL uses $\Delta T = \Delta X$ fixed step method - unsatisfactory.

Define the local errors in \underline{H} and \underline{P} by \underline{leH} and \underline{leP}

Standard error equations in DAE form [Petzold]

$$\begin{bmatrix} -1 - \Delta T \frac{\partial \underline{F}_1}{\partial \underline{\rho H}} & -\Delta T \frac{\partial \underline{F}_1}{\partial \underline{P}} \\ -\Delta T & \Delta T K \end{bmatrix} \begin{bmatrix} \underline{leH} \\ \underline{leP} \end{bmatrix} = \begin{bmatrix} -1 & 0 \\ 0 & 0 \end{bmatrix} \frac{1}{2} \begin{bmatrix} \underline{H}_n - \underline{H}_n^{pred} \\ \underline{P}_n - \underline{P}_n^{pred} \end{bmatrix}$$

This gives $\underline{leH} = K \underline{leP}$ and the standard estimate for the local error:

$$-\Delta T \left(\frac{\underline{leH}}{\Delta T} + \frac{\partial \underline{F}_1}{\partial \underline{\rho H}} \underline{leH} + \frac{\partial \underline{F}_1}{\partial \underline{P}} \underline{leP} \right) = -\frac{(\underline{H}_n - \underline{H}_n^{pred})}{2}$$

Local Error Control Algorithm

Assume zero residuals and applying Taylor's Theorem:

$$E_1 \left(\underline{\tilde{P}}, \underline{\tilde{\rho}\tilde{H}_n}, [\underline{\tilde{\rho}\dot{\tilde{H}}_n}] \right) = \frac{(H_n - H_n^{pred})}{2\Delta T}$$

Solve using multigrid to estimate $\|\underline{leH}\|_\omega = \|\underline{\tilde{H}}_{n+1} - \underline{H}_{n+1}\|_\omega$

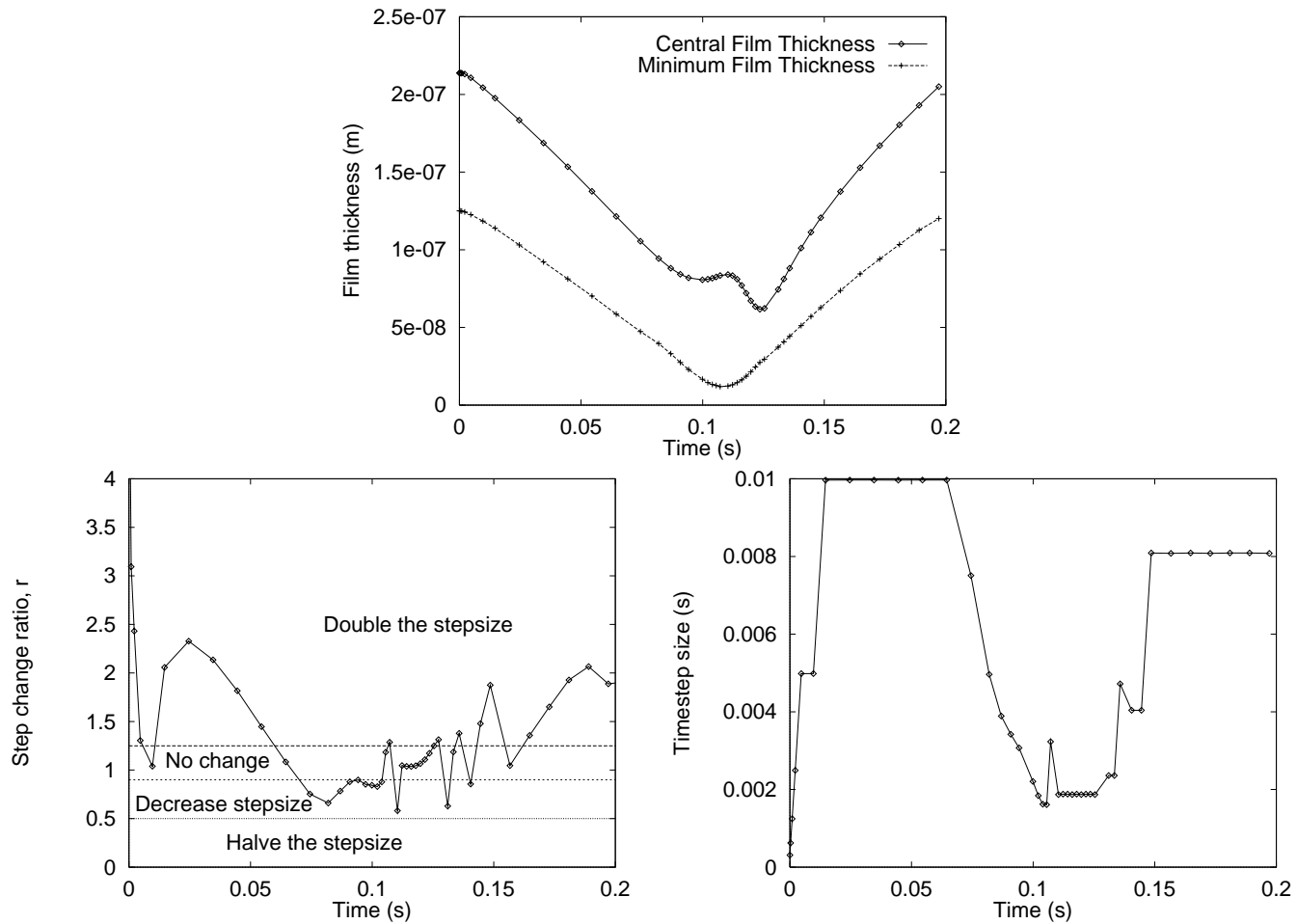
Only use \underline{H} rather than \underline{H} & \underline{P} in error convergence test

Choose TOL to represent estimated spatial error:

$$ATOL = \frac{1}{10} \sqrt{\frac{1}{N_x^C N_y^C} \sum_{I=1}^{N_x^C} \sum_{J=1}^{N_y^C} [\tilde{H}_{i,j} - \tilde{H}_{I,J}]^2}$$

Stepsize ratio, $r = (2 \|\underline{leH}\|_\omega)^{\frac{-1}{k+1}}$

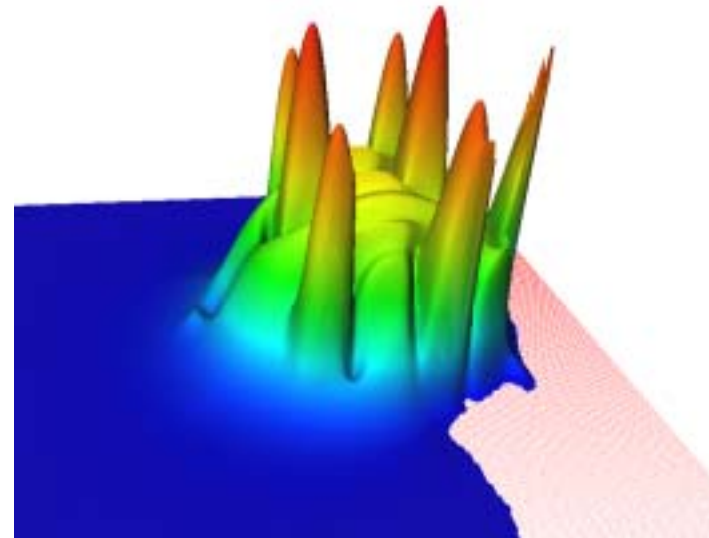
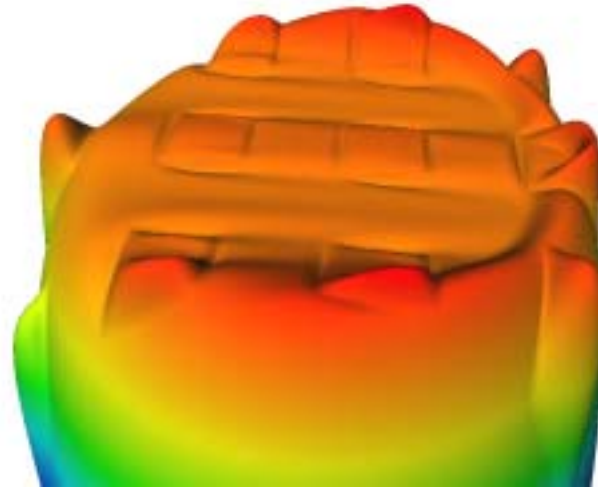
EHL Flow Reversal Using Variable Time Stepping



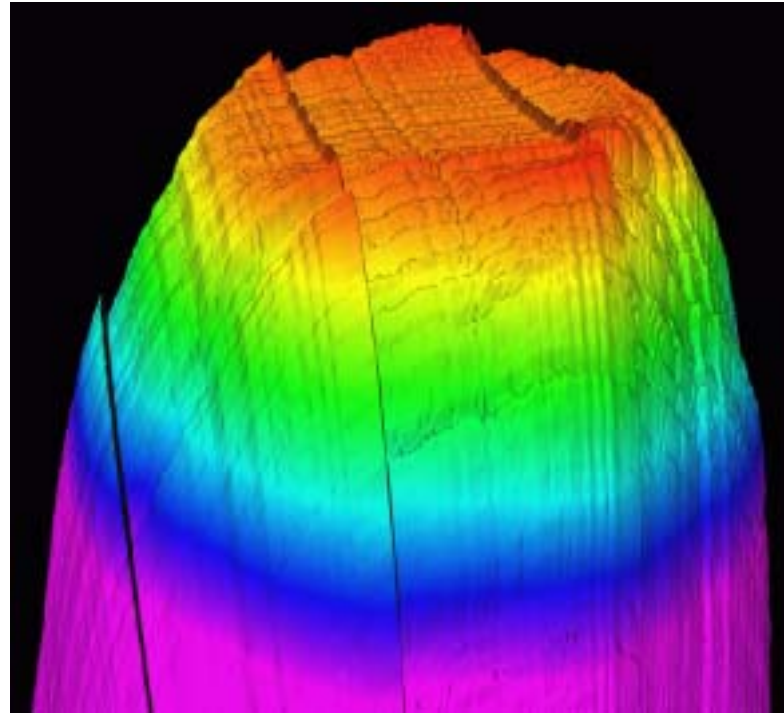
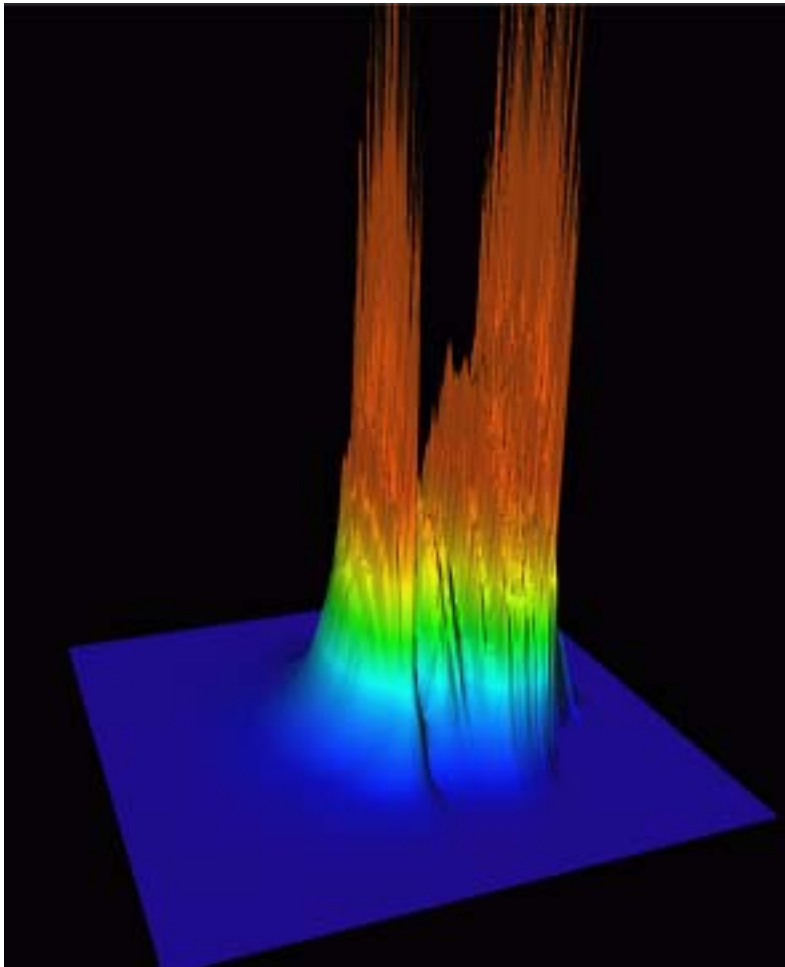
Moving engine parts (e.g. gears) velocity changes sign.

Surface Roughness

- Wear can now be measured
- Detail requires very fine meshes - hence fast solvers
- Important in fields where gap is very narrow
- Many roughness problems *transient*
- Meshes 4000 by 4000 points , 10Gb mem - more required



Real Surface: Pressure + Film Thickness



Future Work

- More adaptive meshing, adjoint approaches in space and time
- Transient rheological models
- Further investigation of more detailed surface features
- Development of large scale parallelism
- Continue PSE IRIS Explorer + SCIRun developments GRID based